



Extension of the non-linear depth imaging capability of the inverse scattering series to multidimensional media: strategies and numerical results

F. Liu, A. B. Weglein, K. A. Innanen and B. G. Nita
Dept. of Physics, University of Houston

Copyright 2005, SBGf - Sociedade Brasileira de Geofísica

This paper was prepared for presentation at the 9th International Congress of the Brazilian Geophysical Society held in Salvador, Brazil, 11-14 September 2005.

Contents of this paper were reviewed by the Technical Committee of the 9th International Congress of the Brazilian Geophysical Society. Ideas and concepts of the text are authors' responsibility and do not necessarily represent any position of the SBGf, its officers or members. Electronic reproduction or storage of any part of this paper for commercial purposes without the written consent of the Brazilian Geophysical Society is prohibited.

Abstract

The inverse scattering series (ISS) has proven, and continues to prove, to be a highly effective formalism for the separate and isolated accomplishment of several key tasks of reflection seismic processing and inversion. In particular, Weglein et al. (2000), Shaw et al. (2003), and Shaw (2005) describe the development of an algorithm distilled from the ISS that concerns itself with the location of subsurface reflectors with no prior knowledge, or related intervening estimation, of the medium wavespeed. The specific non-linear data activity that accomplishes this goal has been investigated by Shaw as such for an idealized 1D pre-stack acoustic experiment; we here describe the extension of those ideas to accommodate media with lateral variation. This is a non-trivial step. Nevertheless, beneath the added algebraic complexity, recognizable patterns and mechanisms are visible. Analysis of these terms and patterns suggests that certain portions of the 2D reflector location mechanisms of the ISS are a good starting point for the creation of algorithms for the accurate depth location of reflectors with a moderate level of lateral variability. The partial 2D imaging capability within the ISS is examined in this paper for the special case of a constant density acoustic medium and taking $kh=0$. We demonstrate numerical implementations of these forms and discuss ongoing work towards capturing further imaging capability residing within the ISS, especially with regards to the accommodation of larger levels of contrast and rapidity of spatial variation in medium properties.

Introduction

The inverse scattering series (ISS) comprises a direct, multidimensional inverse procedure for the reconstruction of an unknown spatial distribution of medium parameters in terms of measurements of a reflected wave field. The formalism prescribes a set of non-linear (or order by order) operations to be carried out upon the data. The history of its investigation as a tool for the processing and inversion of seismic data, and the development of the task-separated treatment of the ISS, is detailed by Weglein et al. (2003). To a remarkable extent, the ISS may be cast to individually carry out what are externally defined to be classical objectives of seismic data processing and inversion: (1) elimination of free surface

multiples, (2) attenuation of internal multiples, (3) location in depth of rapid variations of medium parameters (imaging), and (4) determination of the parameter changes at those locations (inversion). The ISS is an infinite series expansion of the desired output in terms of the data and a chosen (often very simple) reference Green's function, thus each of the above tasks is additionally carried out without an accurate input velocity model.

These task-specific methods are engineered from the ISS through careful study and manipulation of the series components. In this paper we pursue the components of the ISS that, cast appropriately, work on this latter problem, specifically the location in depth of reflectors given only the data and a simple (and highly inaccurate) reference Green's function as input. It is worth noting that in considering this portion and behavior of the ISS, we assume that an amount of pre-processing has occurred: the input to these methods are reflected seismic primaries, in other words the source wavelet, all source and receiver ghosts, and all free surface and internal multiples have been removed.

Our strategy for developing non-linear methods of this kind is to work with the simplest conceivable framework that yet manages to reproduce the aspect of the problem that is of interest; by thus introducing only a single "new" (meaning not yet understood) facet to the problem, one may rationally explain any resulting "new" behavior of the ISS as being a result of that facet. In this paper, we consider the idealized problem of non-linear, ISS-based imaging (Weglein et al., 2000; Shaw et al., 2003) in a single-parameter acoustic medium, as described for the 1D pre-stack case by Shaw (2005), with the added complexity of lateral variability in the unknown medium parameter.

This paper is organized as follows. A brief review of the ISS is followed by a discussion of a form of the linear inverse, given a line source in a homogeneous reference medium. This linear inverse is the input to the higher-order terms of the ISS, which have elsewhere been altered and/or manipulated to separately handle, for instance, internal multiples (e.g., Weglein et al., 1997; Ramirez and Weglein, 2005; Nita and Weglein, 2005), imaging of primaries (Shaw, 2005), inversion of primaries (Zhang and Weglein, 2005), and coupled imaging-inversion (e.g. Innanen, 2003). Here the patterns of the imaging terms of the ISS are investigated; several second-order terms deemed to be responsible for 2D reflector location tasks are presented and described. In the 2D case the imaging-type terms involve cascaded series for correction in depth and lateral coordinates: infinite series, and their closed-forms, for *classes of* (as opposed to *all of*) these 2D imaging terms are also

discussed. We have studied the activity of the 2D imaging engine in the $k_h=0$ setting and in terms of expansions of certain coefficients about a pseudo-laterally-invariant case (i.e., in which a correction similar to the 1D normal incident case (Shaw, 2005) is performed at each lateral location). The lowest order portions of this expansion collapse to a closed-form similar, and reducible, to the 1D normal incidence expression referenced above. This low-order truncation is presumed to be appropriate for Earth models whose difference from the reference model is slowly-varying in the lateral coordinate. When higher order imaging terms, in the same $k_h=0$ setting and with the same low order truncation about the 1D normal incidence case, are considered, the results collapse to the high-order, 1D-normal incidence imaging mechanism described by Innanen (2005). These higher order terms are shown in that reference to better handle large contrast velocity models. We demonstrate the use of these 2D forms on two simple input models that are slowly varying in the lateral coordinate: one involving low-contrast imaging terms similar to those of Shaw (2005) in 1D normal incidence case, and one involving large-contrast imaging terms similar to those developed by Innanen (2005). The success of the imaging terms on data from these models is encouraging; we end with a discussion on continuing extensions of the ideas of this paper.

Background

In operator form, the differential equations describing wave propagation in an actual and a reference medium can be written as

$$LG = -I, \quad L_0 G_0 = -I, \quad (1)$$

where L , L_0 and G , G_0 are the actual and reference differential and Green's operators, respectively, for a single temporal frequency (ω) and I is the identity operator. The above equations assume that the source and receiver signatures have been deconvolved. The perturbation V is defined as $V=L_0-L$. The Lippmann-Schwinger equation, $G=G_0+G_0VG$, may be expanded to form the forward scattering series:

$$G - G_0 = G_0 V G_0 + G_0 V G_0 V G_0 + \dots \quad (2)$$

As described in detail by Weglein et al. (2003), the representation of $V=V_1+V_2+V_3+\dots$ in eqn. (2) as an infinite series in orders of the measured scattered wave field $G-G_0$, gives rise to the ISS when like orders are equated:

$$\begin{aligned} D &= G - G_0 = G_0 V_1 G_0, \\ 0 &= -G_0 V_2 G_0 - G_0 V_1 G_0 V_1 G_0, \\ 0 &= -G_0 V_3 G_0 - G_0 V_1 G_0 V_2 G_0 - G_0 V_2 G_0 V_1 G_0 \\ &\quad - G_0 V_1 G_0 V_1 G_0 V_1 G_0, \end{aligned} \quad (3)$$

etc. By specifying a 1D normal incidence, constant density acoustic reference medium characterized by wavespeed c_0 , and perturbations $V/(\omega/c_0)^2 = \alpha(z)$ on that reference that produce the actual medium $c(z)$, i.e., in

which $\alpha(z) = 1 - c_0^2/c^2(z)$, and through the use of a variety of changes of integration variable and instances of integration by parts, Shaw (2005) identifies a portion of the ISS sum $\alpha = \alpha_1 + \alpha_2 + \alpha_3 + \dots$ that acts to alter the locations of the discontinuities of the linear inverse α_1 (which is in essence the Born approximation, c.f. Cohen and Bleistein, 1979) from the wrong depth to the correct depth. The subseries is:

$$\begin{aligned} \alpha_{IM}(z) &= \sum_{n=0}^{\infty} \frac{(-1/2)^n}{n!} \alpha_1^{(n)}(z) \left(\int_0^z \alpha_1(z') dz' \right)^n \\ &= \alpha_1 \left(z - \frac{1}{2} \int_0^z \alpha_1(z') dz' \right). \end{aligned} \quad (4)$$

The integration by parts analysis exposes and isolates the engine of non-linear imaging, which involves (1) the derivative of the linear inverse with respect to the coordinate in which the reflector location is being corrected, that is (2) weighted by a depth integral of the same linear inverse. We proceed with a study of related forms in the more complex 2D case.

Equations for multidimensional imaging

Eqn. (3) may also be realized for 2D constant density acoustic media, in which the single parameter (cast again as a perturbation on a homogeneous reference medium with wavespeed c_0)

$$\alpha(x, z) = 1 - c_0^2 / c^2(x, z)$$

is the essential quantity. In the corresponding ISS representation $\alpha(x, z) = \alpha_1(x, z) + \alpha_2(x, z) + \alpha_3(x, z) + \dots$, the linear inverse is expressible in terms of the data via the solution of the first equation in (3) as (Clayton and Stolt, 1981):

$$\alpha_1(k_m, k_z) = -\frac{4k_z^2}{k_z^2 + k_m^2} D \left(k_m, \frac{c_0 k_z}{2} \sqrt{1 + \frac{k_m^2}{k_z^2}} \right), \quad (5)$$

in the midpoint conjugate (k_m) and depth conjugate (k_z) domains with the restriction $k_h=0$; the quantity D as it appears may be computed from wave field information on the measurement surface:

$$D(k_m, \omega) = \int_{-\infty}^{\infty} dx_m \int_{-\infty}^{\infty} dt \int_{-\infty}^{\infty} dx_h e^{i(\omega - k_m x_m)} D \left(x_m + \frac{x_h}{2}, x_m - \frac{x_h}{2}, t \right)$$

where the data in the integrand corresponds to $D(x_g, x_s, t)$. With this specific computation of the distribution, in lateral and depth coordinates, of the linear inverse, we turn to higher order terms in the ISS, and express them as operations on $\alpha_1(x, z)$ in analogy to the 1D case. In further analogy to the 1D case we apply an integration-by-parts strategy to extract terms with the imaging-like aspect visible in eqn. (4). Solving the second equation in (3) for $\alpha_2(x, z)$, and manipulating the results accordingly, produces, amongst other terms (Liu et al., 2005):

$$\alpha_{IM2A}(x, z) = -\frac{1}{2} \frac{\partial}{\partial z} \alpha_1(x, z) \int_0^z \alpha_1(x, z') dz' \quad (6)$$

and

$$\alpha_{IM2B}(x, z) = -\frac{1}{2} \frac{\partial}{\partial x} \alpha_1(x, z) \int_0^z \int_0^{z'} \frac{\partial}{\partial x} \alpha_1(x, z'') dz'' dz'. \quad (7)$$

These terms capture much of the behavior intuitively expected from imaging terms at second order for vertical and lateral correction: the first, in eqn. (6), is an exact reproduction of the 1D depth imaging mechanism, involving a first derivative of α_1 with respect to depth weighted by the integral of α_1 down to that depth. The term in eqn. (7), meanwhile (although having no analogous 1D term), has the expected hallmarks of a lateral corrector at second order, involving a first derivative with respect to the *lateral* coordinate, weighted by the depth integral of the rate of change of α_1 . Notice that this term is identically zero if the linear inverse does not vary laterally. We surmise that this term is the first in an infinite series correcting the lateral error in the linear inverse for instances of $k_h=0$.

These results lead to two main conclusions. First, the presence, in the 2D case, of an exact reproduction of the 1D depth imaging engine, as terms that are zero'th order in $\partial\alpha_1/\partial z$ (and the tendency of the imaging terms of the ISS to behave like nested, or cascaded Taylor's series), suggests that we consider the vertical and lateral imaging problem as being akin to a series expansion about the purely vertical imaging problem. Lateral corrector terms that are of low order should be effective when applied to problems involving slow lateral variability; rapid lateral variations will evidently require terms of higher-order in $\partial\alpha_1/\partial x$. Second, this re-appearance of the same patterns as those found in the 1D case allow for the same summations to closed-form that are in place in 1D scenarios. Hence, the zero'th order lateral corrector, and infinite order depth corrector expression for the 2D case is (*c.f.* eqn. (4)):

$$\alpha_{LOIS}(x, z) = \alpha_1 \left(x, z - \frac{1}{2} \int_0^z \alpha_1(z') dz' \right). \quad (8)$$

We refer to this quantity as LOIS to conform with descriptions of the 1D imaging algorithm as the "leading-order imaging subseries" (leading order referring to the fact that the subseries coefficients are approximated as the integral of the first power of α_1 only (Shaw, 2005)). As in Shaw's analysis, we consider eqn. (8) to be appropriate for media of low but spatially sustained contrast; a depth corrector that involves the same engine as in the 1D case, but with a different quantity under scrutiny at each x . In contrast, inclusion of a larger cohort of ISS imaging terms, which Innanen (2005) describes as the incorporation of a geometric series in α_1 into the integrands of the coefficients of eqns. (4) and (8), leads to a second expression

$$\alpha_{HOIS} \left(x, z + \frac{1}{2} \int_0^z \frac{\alpha_1(z')}{1 - 0.25\alpha_1(z')} dz' \right) = \alpha_1(x, z) \quad (9)$$

that we consider to be appropriate for larger contrast media (and hence we refer to as HOIS). The exchange of input and output variables has the empirically useful effect of changing the integration limits in (9) (Liu et al., 2005). In the following we test both expressions numerically.

To summarize: manipulation of the 2D ISS equations in the case of a single-parameter acoustic medium leads to several imaging-like terms. Some are identical to the 1D case, and thus may be summed to closed form. Others have no 1D counterpart, and are currently interpreted as low-order terms correcting for lateral errors in reflector location. Since the 2D imaging terms appear to treat the lateral/vertical problem as an expansion about the vertical problem, we expect the closed-form depth-imaging expressions (8) and (9) to be appropriate for instances of smooth lateral variation in the *difference* between the actual perturbation $\alpha(x,z)$ and the linear inverse $\alpha_1(x,z)$.

Numerical examples

We present some simple and illustrative examples of the "low lateral order" 2D imaging algorithms of eqns. (8) and (9). Figs. 1 and 2 illustrate the acoustic single parameter models we consider, and Figs. 3 and 4 illustrate example shot records from the synthetic data sets derived from these models. The models chiefly differ in their levels of medium contrast, with Fig. 1 a relatively low-contrast example and Fig. 2 a large-contrast example. The data is created using a fourth-order finite difference scheme, with a temporal sampling rate of $2ms$ and a lateral spatial sampling rate of $5m$. The source signature is the first derivative of a Gaussian with a peak frequency of $28Hz$. The resultant data are used as described above to compute the linear inverse associated with a homogeneous reference medium of wavespeed $c_0=1500m/s$. These linear outputs are illustrated in Figs. 5 and 6 (on the left panels) for the low- and high-contrast cases respectively. The lateral variation in the top interface, and the presence of a sustained difference between the actual and the reference media in general, can be readily seen to negatively influence the locations of the deeper reflectors in these linear results. The task of the non-linear imaging mechanism is to correct the locations of these reflectors laterally and vertically, although by design the lateral error is very smooth in these examples. The correct locations of the horizons are illustrated in red.

Figs. 5 and 6 (on the right panels) demonstrate the effect of implementing eqn. (8) on the linear input (seen on the left). In Fig. 5, the aberrant lateral variation in the lower reflectors seen in the linear inverse has been largely corrected for as has the bulk depth error. However, in the large-contrast case in Fig. 6 the results of eqn. (8), i.e. LOIS, are less successful in performing the requisite correction, which is clearly more "intensive". The high-order imaging mechanism of eqn. (9) is brought to bear on the problem in Fig. 7, in which we see a return to the highly satisfactory corrective nature of the non-linear imaging, both in correcting the bulk depth error of the

reflectors and in flattening the erroneous lateral variation of the lower interfaces.

Conclusions

We present the first results of an extension of the velocity-independent imaging methods of the ISS to accommodate media that vary laterally as well as in depth. In spite of the added complexity of the ISS terms, the use of an integration-by-parts thinking produces classes of terms that either reproduce precisely the depth corrective terms of the 1D normal incidence case, or have the hallmarks of being part of a laterally corrective mechanism. Both classes of terms call for specific and reasonably straightforward non-linear data activity, that (as shown for a low-order approximation in the lateral correction and appropriate Earth models) we demonstrate has an extremely encouraging impact on 2D synthetic data. Ongoing research is geared towards moving beyond current simplifying restrictions, e.g. fixed $k_{\text{r}}=0$, and the incorporation of only low-order lateral correction terms.

Acknowledgments

The authors are grateful to Simon Shaw, Haiyan Zhang, Einar Otnes, and the sponsors and personnel of M-OSRP.

References

- Clayton, R.W. and Stolt, R.H., *A Born-WKB inversion method for acoustic reflection data*, 1981: Geophysics 46 No. 11, 1559-1567.
- Cohen, J.K. and Bleistein, N., *Velocity inversion procedure for acoustic waves*, 1979: Geophysics 44 No. 6, 1077-1087.
- Innanen, K.A., *Methods for the treatment of acoustic and absorptive/dispersive wave field measurements*, 2003: Ph.D. Thesis, University of British Columbia.
- Innanen, K.A., *Two non-linear forward and inverse approximations for wave fields in the presence of sustained medium perturbations*, 2005: In preparation.
- Liu, F., Weglein, A.B., Innanen, K.A., and Nita, B.G., *Inverse scattering series for vertically and laterally varying media: application to velocity-independent depth imaging*, 2005: M-OSRP04 Annual Report.
- Nita, B.G. and Weglein, A.B., *Inverse scattering internal multiple attenuation algorithm in complex multi-D media: the pseudo-depth/vertical time monotonicity condition and higher-dimension analytic analysis*, 2005: submitted to Inverse Problems.
- Ramirez, A. and Weglein, A.B., *Progressing the analysis of the phase and amplitude prediction properties of the inverse scattering internal multiple attenuation algorithm*, 2005: Journal of Seismic Exploration, accepted for publication.
- Shaw, S.A., Weglein, A.B., Foster, D.J., Matson, K.H. and Keys, R.G., *Convergence properties of a leading-order depth imaging series*, 2003: Soc. Expl. Geophys., Expanded Abstracts
- Shaw, S.A., *An inverse scattering series algorithm for depth imaging of reflection data from a layered acoustic medium with an unknown velocity model*, 2005: Ph.D. Thesis, University of Houston.
- Weglein, A.B., Gasparotto, F.A., Carvalho, P.M. and Stolt, R.H., *An inverse-scattering series method for attenuating multiples in seismic reflection data*, 1997: Geophysics 62 No. 6, 1975-1989.

Weglein, A.B., Matson, K.H., Foster, D.J., Carvalho, P.M., Corrigan, D., and Shaw, S.A., *Imaging and inversion at depth without a velocity model: theory, concepts, and initial evaluation*, 2000: Soc. Expl. Geophys., Expanded Abstracts.

Weglein, A.B., Araujo, F.V., Carvalho, P.M., Stolt, R.H., Matson, K.H., Coates, R.T., Corrigan, D., Foster, D.J., Shaw, S.A. and Zhang, H., *Topical review: inverse scattering series and seismic exploration*, 2003: Inverse Problems 19, R27-R83

Zhang, H. and Weglein, A.B., *The inverse scattering series for tasks associated with primaries: depth imaging and direct non-linear inversion of 1D variable velocity and density acoustic media*, 2005: In preparation.

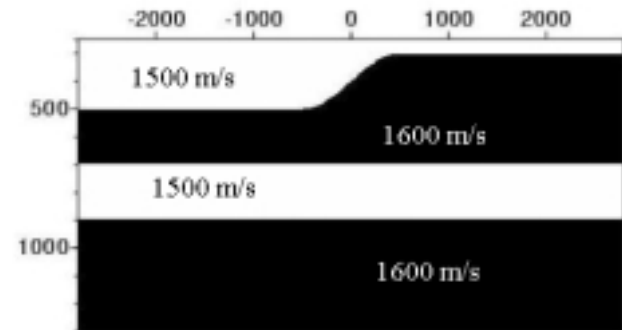


Figure 1. First input model for numerical testing of 2D non-linear imaging algorithm. Top interface has a spatial variation designed to produce lateral and vertical error in the locations of reflectors predicted by the linear inverse and a homogeneous reference medium. Contrasts of moderate magnitude are chosen.

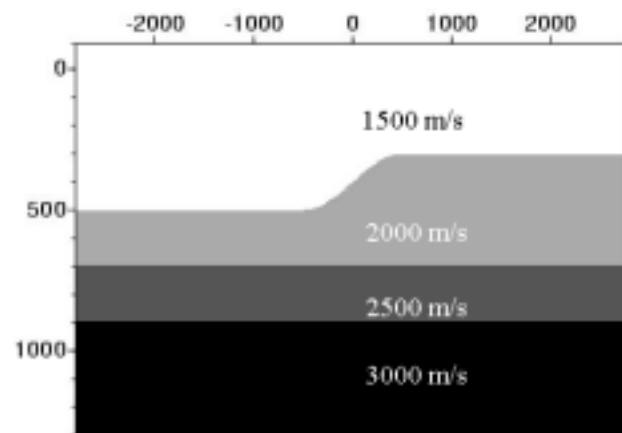


Figure 2. Second input model for numerical testing of 2D non-linear imaging algorithm. Again, the top interface is designed to produce specific lateral and vertical error in the linearly-computed locations of the deeper horizons, given a homogeneous reference medium. Contrasts of large magnitude are chosen.

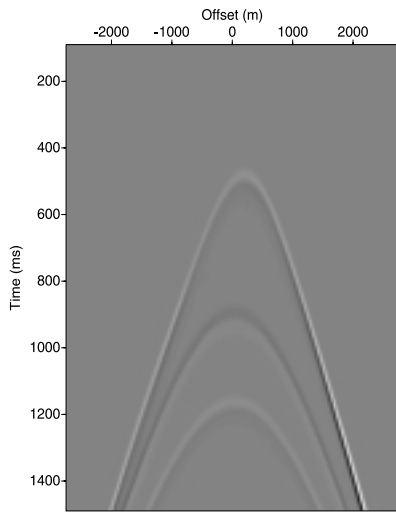


Figure 3. An example single shot record from synthetic data, generated over model 1 (Fig. 1). Fourth-order finite difference scheme utilized.

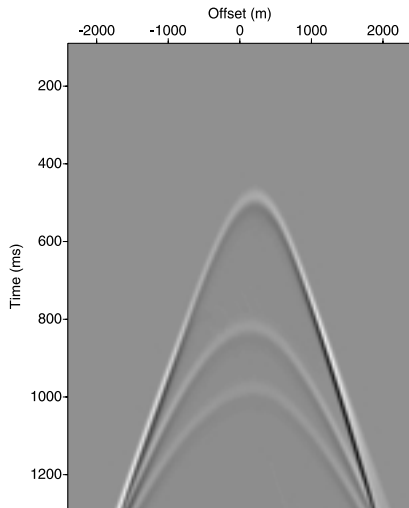


Figure 4. An example single shot record from synthetic data, generated over model 2 (Fig. 2). Fourth-order finite difference scheme utilized.

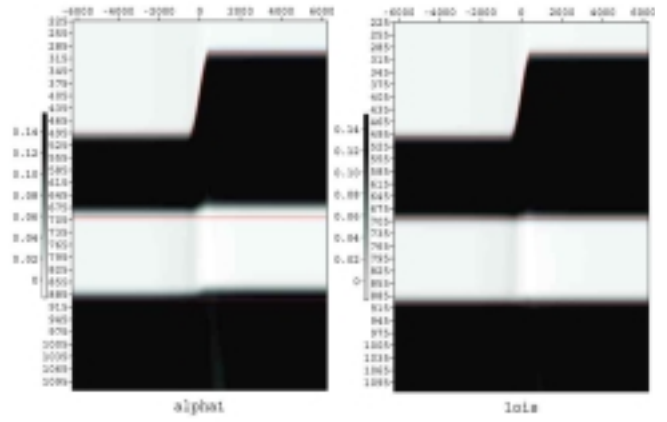


Figure 5. Left panel: linear inverse with homogeneous wavespeed, computed from synthetic data over model 1 (Fig. 3). Lateral and vertical errors in reflector locations are visible when compared to actual horizon depths (red). Right panel: LOIS enacted on the linear input, via eqn. (8) with accurate results.

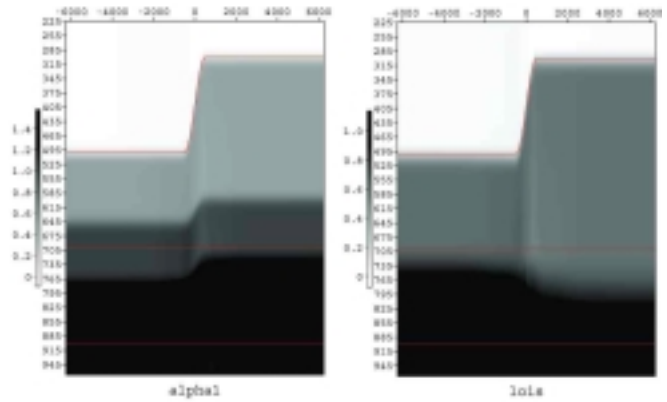


Figure 6. Left panel: linear inverse with homogeneous wavespeed, computed from synthetic data over model 2 (Fig. 4). Lateral and vertical errors in reflector locations are visible when compared to actual horizon depths (red). Right panel: LOIS enacted on the linear input, via eqn. (8) with inaccurate results.

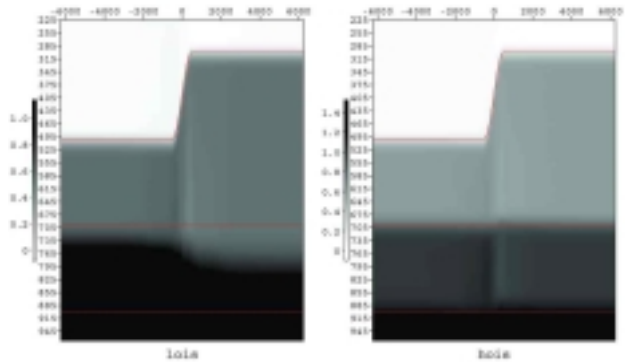


Figure 7. Model 2 revisited. Left panel: LOIS enacted on the linear input, via eqn. (8) with inaccurate results. Right panel: HOIS enacted on the linear input, via eqn. (9), with accurate results.